



Published as: *Arch Biochem Biophys.* 2006 April 15; 448(1-2): 31–44.

Stereochemistry and deuterium isotope effects associated with the cyclization-rearrangements catalyzed by tobacco epiaristolochene and hyoscyamus premnaspirodiene synthases, and the chimeric CH₄ hybrid cyclase

David J. Schenk^{a,1}, Courtney M. Starks^{b,2}, Kathleen Rising Manna^c, Joe Chappell^c, Joseph P. Noel^b, and Robert M. Coates^{a,*}

^a Department of Chemistry, University of Illinois, 600 South Mathews Ave., Urbana, IL 61801, USA

^b Howard Hughes Medical Institute, Jack H. Skirball Center for Chemical Biology and Proteomics, Salk Institute for Biological Studies, 10010 North Torrey Pines Rd., La Jolla, CA 92037, USA

^c Department of Plant and Soil Sciences, University of Kentucky, Lexington, KY 40546-0091, USA

Abstract

Tobacco epiaristolochene and hyoscyamus premnaspirodiene synthases (TEAS and HPS) catalyze the cyclizations and rearrangements of (*E,E*)-farnesyl diphosphate (FPP) to the corresponding bicyclic sesquiterpene hydrocarbons. The complex mechanism proceeds through a tightly bound (*R*)-germacrene A intermediate and involves partitioning of a common eudesm-5-yl carbocation either by angular methyl migration, or by C-9 methylene rearrangement, to form the respective eremophilane and spirovetivane structures. In this work, the stereochemistry and timing of the proton addition and elimination steps in the mechanism were investigated by synthesis of substrates bearing deuterium labels in one or both terminal methyl groups, and in the pro-*S* and pro-*R* methylene hydrogens at C-8. Incubations of the labeled FPPs with recombinant TEAS and HPS, and with the chimeric CH₄ hybrid cyclase having catalytic activities of both TEAS and HPS, and of unlabeled FPP in D₂O, together with gas chromatography–mass spectrometry (GC–MS) and/or NMR analyses of the labeled products gave the following results: (1) stereospecific CH₃ → CH₂ eliminations at the *cis*-terminal methyl in all cases; (2) similar primary kinetic isotope effects (KIE) of 4.25–4.64 for the CH₃ → CH₂ eliminations; (3) a significant intermolecular KIE (1.33 ± 0.03) in competitive cyclizations of unlabeled FPP and FPP-*d*₆ to premnaspirodiene by HPS; (4) stereoselective incorporation of label from D₂O into the 1β position of epiaristolochene; (5) stereoselective eliminations of the 1β and 9β protons in formation of epiaristolochene and its Δ¹⁽¹⁰⁾ isomer epieremophilene by TEAS and CH₄; and (6) predominant loss of the 1α proton in forming the cyclohexene double bond of premnaspirodiene by HPS and CH₄. The results are explained by consideration of the conformations of individual intermediates, and by imposing the requirement of stereoelectronically favorable proton additions and eliminations.

Keywords

Sesquiterpenes; Eremophilanes; Spirovetivane; Germacrane; Enzyme mechanisms; Stereochemistry; Deuterium labeling; Isotope effects; Rearrangements; Cyclizations; Carbocations

*Corresponding author: Fax: +1 217 244 8024. coates@scs.uiuc.edu (R.M. Coates).

¹Present address: Department of Drug Metabolism, Merck Research Laboratories, RY80R-104, P.O. Box 2000, Rahway, NJ 07065, USA.

²Present address: Monsanto Company, 800 N. Lindbergh Blvd., Creve Coeur, MO 63167, USA.

Tobacco epiaristolochene and hyoscyamus premnaspirodiene synthases (TEAS³ and HPS) [1,2] are terpene cyclases responsible for the production of the respective sesquiterpene hydrocarbons (**2** and **5**) in the biosynthesis of the oxygenated phytoalexins capsidiol (**4**), solavetivone (**6**), lubimin (**7**), rishitin (**8**), and related metabolites in sweet pepper, tobacco, potato, and other Solanaceae (Scheme 1) [3–5].

Incorporation of [1,2-¹³C₂]acetate into capsidiol in *Capsicum annum* cultures and NMR analyses confirmed the occurrence of a methyl migration in the biosynthesis of this eremophilane sesquiterpene [6]. Retention of deuterium at C4 of capsidiol biosynthesized from [4,4-²H₂]mevalonate demonstrated that the unusual *trans*-stereochemistry of the vicinal methyl groups could not be attributed to epimerization of a *cis*-eremophilane precursor [7].

The hydrocarbon intermediate isolated from elicitor-treated cell cultures of *Nicotiana tobacum* [8] was identified as (+)-epiaristolochene (**2**) by comparison with the diene prepared chemically by deoxygenation of capsidiol [9], the structure and stereochemistry of which were established by an X-ray crystallo-graphic analysis [10]. Kinetic analysis of the oxidation of **2** to capsidiol and the potential intermediates epiaristolochene-1 β - and -3 α -ol with the cytochrome P₄₅₀ oxidase epiaristolochene dihydroxylase (EAH) established the preferred order of the oxidation steps, **2** \rightarrow **3** \rightarrow **4** [11,12]. The sequence of oxidative transformations and intermediates in the conversion of solavetivone to lubimin and rishitin was elucidated by incorporation of deuterium and carbon-13 labeled precursors [13–15]. The presumed sesquiterpene precursor (–)-premnaspirodiene (**5**) [16] has been synthesized as the pure enantiomer [17] and in racemic form [18], and its identification as the product of HPS rests primarily on GC–MS evidence [19].

The usual mechanism for the closely related processes catalyzed by TEAS and HPS are presented in Scheme 2 [1,2]. Intramolecular alkylation of the terminal double bond of the FPP substrate generates the enzyme bound germacrene A intermediate (**9**). Proton-induced cyclization of **9** in a boat-chair conformation leads to a 5,10-*syn* eudesmyl ion **10A** that undergoes 5 \rightarrow 4 hydride shift to form the branch point intermediate **10B**. 1,2-Methyl migration followed by proton elimination give rise to epiaristolochene (**2**) and epieremophilene (**13**), whereas ring contraction by C-9 methylene rearrangement and elimination produces premnaspirodiene (**5**).

The cloning and over-expression of recombinant TEAS and HPS in *Escherichia coli* provided sufficient quantities of these interesting cyclases for structural and mechanistic investigations [20]. These two proteins are 77% identical and 81% similar based on amino acid sequence alignment, contain the familiar DDXXD aspartate triad linked to diphosphate binding, and have kinetic characteristics typical of terpene cyclases. One of a series of chimeric proteins resulting from domain swapping designated CH₄ catalyzed the conversion of **1** to epiaristolochene, premnaspirodiene, and an unknown product subsequently identified as epieremophilene (**13**), i.e., the $\Delta^{1(10)}$ isomer of **2** [11,21]. Pre-steady state kinetic data are consistent with either a rate-determining cyclization to the germacrene A intermediate or final dissociation of the bicyclic products, and the existence of a single catalytic site on the CH₄ hybrid enzyme [22]. X-ray diffraction analysis of crystalline TEAS in the absence and presence of inert substrate mimics revealed a hydrophobic, aromatic-rich binding pocket in the C-

³Abbreviations used: SCS, School of Chemical Sciences at the UI; THF, tetrahydrofuran; DMSO, dimethyl-sulfoxide; DMF, *N,N*-dimethylformamide; TLC, thin-layer chromatography; NMR, nuclear magnetic resonance; NOE, nuclear Overhauser effect; Hz, Hertz; GC, gas chromatography; MS, mass spectrum; FAB, fast atom bombardment; *m/z*, mass/charge ratio; PP, diphosphate; FPP, farnesyl diphosphate; pyr., pyridine; 18-C-6, 18-crown-6 ether; Bn, benzyl; Ms, methanesulfonyl; Me, methyl; Et, ethyl; Ph, phenyl; NMO, *N*-methylmorpholine *N*-oxide; TEAS, tobacco epiaristolochene synthase; HPS, hyoscyamus premnaspirodiene synthase; CH₄, chimeric cyclase construct; KIE, kinetic isotope effect; satd, saturated.

terminal domain with two Mg^{2+} ions positioned near the opening [23]. The production of germacrene A (**9**) by the point mutant TEAS-Y520-F confirmed the identity of the macrocyclic intermediate and a role for tyrosine 520 in catalysis, perhaps in contributing to an H-bonding network making up the back of the active site pocket [24].

The functionally similar aristolochene synthases isolated from the fungi *Aspergillus terreus* and *Penicillium roquaforti* catalyze the conversion of FPP to the 4β - CH_3 , 7α -isopropenyl diastereomer of **2** [1,2]. However, the amino acid sequences of these fungal cyclases differ appreciably from those of TEAS and HPS. Labeling experiments established that the macrocyclization step occurs with inversion at C-1 of the substrate and proton elimination at the *cis*-terminal methyl position, and that conversion of the enzyme-bound intermediate to aristolochene takes place with $10 \rightarrow 5$ methyl migration and *syn*-related proton elimination [25,26]. Indirect evidence supporting the same germacrene A intermediate (**9**) was obtained by enzyme-catalyzed cyclization of (*7R*)-6,7-dihydro FPP to 6,7-dihydro germacrene A [27].

The objectives of the present work were to analyze the timing of the cyclization steps and the stereochemistry of the individual protonation and deprotonation events in the mechanism by means of deuterium labeling. In this paper, we report syntheses of farnesyl PPs bearing deuterium in the terminal methyl groups and in the pro-R and pro-S positions at C-8. The stereochemistry of proton transfer steps was elucidated by GC-MS and/or NMR analyses of the products from incubations of the labeled substrates with the three enzymes and from incubations conducted in D_2O . Comparisons of the isotope effects and stereospecificities of the different reactions catalyzed by TEAS, HPS, and CH_4 afford new insights on the positions of active site acids and bases, on the determinants of product specificity, and on the rate determining steps.

Materials and methods

Analytical methods

1H , 2H , ^{13}C , and ^{31}P NMR spectra were recorded with Varian U400, U500, U500NB or Unity Inova 750NB spectrometers in the SCS NMR Spectroscopy Facility at the University of Illinois. The following solvents and reference values in ppm were used in obtaining the NMR data: $CDCl_3$ (1H , 7.26; 2H , 7.26; ^{13}C : 77.0), benzene- d_6 (1H , 7.16; 2H , 7.16; ^{13}C , 128), $THF-d_8$ (1H , 1.73). ^{31}P NMR spectra were externally referenced to 0 ppm with 85% H_3PO_4 . Chemical shifts are in ppm, and coupling constants are in Hertz. NOE spectra were generally recorded after at least three freeze-thaw cycles performed in standard 5-mm NMR tubes. NOE data are reported in the following format: data (MHz, solvent): irrad. (ppm irradiated), obs. δ (data). Mass spectra were recorded on Micromass 70V-SE instruments with either probe or HP 5890 GC inputs. The isotopic contents were calculated with the MATRIX program in the SCS Mass Spectroscopy Laboratory at the UIUC to correct for the isotope distributions and the contributions from natural abundance carbon 13. GC analyses were carried out on a Shimadzu Model 14-A GC with a Rt_x -5 30-m fused silica capillary column. The MS fragmentation data were determined from EI (70 eV) mass spectra unless otherwise noted.

Purification and characterization

Organic starting materials and stable intermediates shown in Schemes 3 and 4 were purified in most cases by flash chromatography on silica gel 60 (230–400 mesh ASTM) from Merck [28]. TLC analyses were performed on 250- μm silica gel F254 pre-coated plates. TLC visualizations were performed with 5% phosphomolybdic acid (0.2 M in 2.5% conc. H_2SO_4 /EtOH (v/v)), I_2 , or anisaldehyde (2.5% (v/v), 1% HOAc, and 3.4% conc. H_2SO_4 in ethanol). The purity of purified intermediates was judged to be ≥ 90 –95% by TLC and/or GC analyses and NMR spectra. The deuterium content of labeled intermediates in Schemes 3 and 4 was

determined by GC–MS analyses as described above. The position of the label was verified by peaks absent in ^1H NMR spectra and often also directly from ^2H NMR spectra.

Reagents and starting materials

Methyl 2-(bis (2,2,2-trifluoroethyl)phosphono)propionate (See Scheme 3) was prepared by methylation of the corresponding phosphonoacetate (NaH, DMSO, methyl 2-(bis-2(2,2,2-trifluoroethyl)phosphono)acetate, CH_3I ; 25 °C, 5 days, 3.33 g, 64%) [29]. A similar reaction with CD_3I gave the labeled phosphonopropionate reagent: 2.98 g (53%). (*E,E*)-Farnesyl benzyl ether was prepared as described for geranyl benzyl ether (KH, THF, (*E,E*)-farnesol, benzyl bromide, 70 °C, 16 h; 99, 96% purity) [30]. Aldehyde ether **14** was prepared from farnesyl benzyl ether by the following four steps [31,32]: (a) regioselective hypobromination of the 9,10 double bond (NBS, aq THF, 0 °C, 4.5 h, 76%); (b) conversion to the 9,10 epoxide (powdered KOH, ether, 6 h, 25 °C, 98%) [33]; (c) hydrolysis to the 9,10 diol (70% HClO_4 , aq THF, 25 °C, 1.5 h, 91% unpurified); (d) oxidative cleavage to aldehyde **14** (NaIO_4 , aq THF, 5 h, 25 °C, 76%).

Synthesis of deuterium-labeled farnesyl diphosphates

The 7-step synthesis of farnesyl PPs bearing deuterium in one or both terminal CH_3 groups from aldehyde **14** is outlined in Scheme 3. *Z*-Selective olefinations with Still's trifluoroethyl phosphono-propionates [34] followed by AlD_3 reductions [35] of *cis*-ester **15** afforded the *cis*-deuterio hydroxy ethers **16-*d*₂** and **16-*d*₅**. The key reaction was the reductive substitution effected by first activation as the allylic phosphates **17** [31,36] followed by hydride and deuteride displacements with lithium triethylborohydride and triethylborodeuteride to give labeled farnesyl ethers **18-*d*₂**, **18-*d*₃**, and **18-*d*₆**. The allylic phosphate intermediates proved to be stable to chromatography and prolonged storage in a freezer. Cleavage of the benzyl ether was accomplished by Li-NH_3 reductions to form the respective labeled (*E,E*)-farnesols, [$13,13\text{-}^2\text{H}_2$]-, [$13,13,13\text{-}^2\text{H}_3$]-, and [$12,12,12,13,13,13\text{-}^2\text{H}_6$]**19**. The positional integrity of the deuterium labels was determined from their ^1H and ^2H NMR spectra in benzene-*d*₆. Representative preparative procedures and characterization data for [$12,12\text{-}^2\text{H}_2$]farnesol are described in detail below. Procedures and data for other intermediates and labeled compounds reported may be found in a PhD dissertation [37]. (*2E,6E,10Z*)-[$13, 13\text{-H}_2$] 1-benzyloxy-3,7,11-trimethyl-2,6,10-dodecatriene, (*2E,6E,10Z*)-[$13,13\text{-}^2\text{H}_2$] farnesyl benzyl ether (**18-*d*₂**) The general method of Welch was followed [31,36]. A solution of 0.291 g (0.88 mmol) of **16-*d*₂** and 0.085 mL (0.83 g, 1.1 mmol) of pyridine in 4 mL of CH_2Cl_2 was stirred and cooled at 0 °C as diethyl chlorophosphate (0.14 mL, 0.16 g, 0.93 mmol) was added. After 1.5 h, 30 mL of ether was added. The ether solution was washed with 1% HCl (3 × 20 mL), satd. NaHCO_3 (1 × 10 mL), and satd. NaCl (1 × 10 mL); dried (Na_2SO_4); and concentrated. Purification by column chromatography on silica gel (2:1 hexane/ethyl acetate) provided 0.269 g (66%) of diethyl phosphate **17** as a clear oil. The purity of the diethyl phosphate was estimated to be >95% by ^1H NMR analysis. Data for the diethyl phosphate: TLC R_f 0.23 (2:1 hexane/ethyl acetate); ^1H NMR(500 MHz, CDCl_3) δ 7.34(m, 4H, aryl H), 7.28(m, 1H, aryl H), 5.40(t of sextets, 1H, $J = 7.3, 1.5$ Hz, =CH), 5.37(td, 1H, $J = 7.3, 0.8$ Hz, =CH), 5.11(t of sextets, 1H, $J = 6.8, 1.3$ Hz, =CH), 4.50(s, 2H, OCH_2Ar), 4.11(q, 4H, $J = 7.3$ Hz, CH_3CH_2), 4.03(d, 2H, $J = 6.5$ Hz, CHCH_2O), 2.13(m, 4H, CH_2), 2.04(m, 2H, CH_2), 1.99(m, 2H, CH_2), 1.77(q, 3H, $J = 1.5$ Hz, CH_3), 1.65(s, 3H, CH_3), 1.59(s, 3H, CH_3), 1.33(td, 6H, $J = 7.2, 0.7$ Hz, CH_2CH_3); ^2H NMR(77 MHz, CDCl_3) δ 4.51(s, CCD_2).

A solution of 0.115 g (0.246 mmol) of the above diethyl phosphate in 10 mL of THF was stirred and cooled at 0 °C as 1.4 mL (1 M, 1.4 mmol) of LiBEt_3H in THF was added. After 45 min, 3 mL of 1 N HCl and 6 mL H_2O were added, and the product was extracted with pentane (3 × 15 mL) and ether (2 × 15 mL). The combined organic layers were washed with 25 mL of H_2O and 25 mL of satd. NaCl, dried (MgSO_4), and concentrated at reduced pressure.

Purification by chromatography on silica gel (50:1 hexane/ethyl acetate) provided 55.4 mg (72%) of [13,13-²H₂]farnesyl benzyl ether (**18-d₂**) as a clear colorless oil. The purity was estimated to be >95% by ¹H NMR analysis. The ¹H NMR data for **18-d₂** are similar to those for unlabeled farnesyl benzyl ether except for the following: ¹H NMR(500 MHz, CDCl₃) δ 5.40(t of sextets, 1 H, *J* = 6.5, 1.0 Hz, =CH), 1.67(d, 3H, *J* = 1.5 Hz, CH₃), 1.65(s, 3H, CH₃), 1.61(s, 1H, CD₂H), 1.60(s, 3H, CH₃); ²H NMR(77 MHz, CDCl₃) δ 1.59(d, *J* = 2.2 Hz, CD₂H). (2*E*,6*E*,10*Z*)-[13,13-²H₂]Farnesol(**19-d₂**). The procedure followed one in the literature [35]. [13,13-²H₂]Farnesyl benzyl ether (0.0554 g, 0.175 mmol) prepared by phosphate reduction in 5 mL of THF was added to a stirred suspension of 0.060 g (8.64 mmol) of Li rod pieces in 25 mL of NH₃ at -78 °C. After 1 h, several drops of 3-hexyne were added, the CO₂/isopropyl alcohol bath was removed, MeOH (30 mL) was slowly added, and the majority of the NH₃ was removed with a gentle stream of N₂. Hexane (20 mL) and 1% HCl (20 mL) were added. The aqueous layer was extracted with hexane (3 × 20 mL) and CH₂Cl₂ (3 × 20 mL), and the combined organic layers were washed with satd. NaHCO₃ (2 × 100 mL) and satd. NaCl (1 × 100 mL), dried (MgSO₄), and concentrated. Chromatography on silica gel (8:1 hexane/ethyl acetate) afforded 0.0279 g (71%) of farnesol-*d₂* (**19-d₂**) as a colorless oil. ²H NMR and MS analyses showed that **18-d₂** possessed deuterium only in the *cis*-methyl position, and the label content was 99.0% *d₂*, and 0.5% *d₁*. GC and ¹H NMR analyses determined the purity to be 97.6%. The ¹H NMR data are similar to those of unlabeled farnesol. Data for **19-d₂**: TLC *R_f* 0.13 (8:1 hexane/ethyl acetate); ¹H NMR(500 MHz, benzene-*d₆*) δ 5.39(t, 1H, *J* = 6.8 Hz, =CH), 5.23(t, 2H, *J* = 6.3 Hz, =CH), 3.97(d, 2H, *J* = 6.5 Hz, CH₂OH), 2.17(m, 2H, CH₂), 2.10(m, 4H, CH₂), 1.99(m, 2H, CH₂), 1.68(s, 3H, CH₃), 1.58(s, 3H, CH₃), 1.53(s, 1H, CD₂H), 1.47(s, 3H, CH₃); ²H NMR(77 MHz, benzene-*d₆*) δ 1.51(d, *J* = 2.1 Hz, CD₂H); MS (EI) *m/z* 225(16.6), 224(M⁺, 100), 223(2.7); 99.0% *d₂*, 0.5% *d₁*.

Other methods for effecting the reduction of the dideuterio alcohol **16-d₂** to **18-d₂** and **18-d₃** were evaluated. Although, the two-step sequence (a) SO₃, pyridine, [38,39] (b) LiBET₃H and LiBET₃D gave labeled products without any loss of positional integrity, it proved difficult to monitor the initial step by TLC owing to rapid hydrolysis of the sulfate salt on silica gel, and the sulfate salt was quite unstable. Conversion to the allylic mesylate (CH₃SO₂Cl, Et₃N, CH₂Cl₂, 0 °C) and reductive displacement with LiBET₃H and LiBET₃D (THF-CH₂Cl₂) was also tried. Although this method was successful in the preparation of [16,16,16-²H₃](*E,E,E*)-geranylgeranyl benzyl ether bearing deuterium in the *trans*-terminal methyl group [32], the same reactions on *cis*-dideuterio alcohol **16-d₂** afforded **17-d₂** as a 3:1 mixture of *cis*- and *trans*-isomers. Evidently the less stable *cis*-mesylate undergoes partial isomerization to the *trans* form during one or both reactions.

(*S*)- and (*R*)-[8-²H₁]Farnesyl PPs bearing deuterium in the prochiral methylene at C-8 were synthesized from aldehyde **20** [35] as shown in Scheme 4 to elucidate the stereochemistry of the proton elimination step forming the double bond of epiaristolochene. *E*-Selective Wittig olefination and AID₃ reduction afforded **22-d₂**. The deuterated aldehyde resulting from ruthenate oxidation underwent enantioselective reductions with (*R*)- and (*S*)-alpine borane in moderate yield. The enantiomeric excesses of the resulting labeled alcohols, (*S*)- and (*R*)-**23-d₁**, were determined to be 90.4 and 99% by NMR analyses of their camphanate derivatives [40–42]. Biellmann coupling reactions between excess lithio dimethylallyl *p*-tolyl sulfone [43] and the allylic phosphates (3:1 THF-HMPA, -20 °C, 18 h) provided sulfonyl ethers (*R*)- and (*S*)-**24-d₁**. Simultaneous reductive cleavage of the allylic sulfone and the benzyl ether afforded (*S*)- and (*R*)-[8-²H₁]farnesols **19** (100% *d₁*) by GC–MS analyses. In the absence of any obvious way to determine the stereochemistry of the label, we assume predominant inversion occurred in the C–C bond forming reaction like a similar Biellmann coupling employed in the synthesis of (*R*)-[4-²H₁]geranylgeraniol [32].

The labeled farnesols were converted to the diphosphates by formation of the allylic chlorides [44] followed by S_N2 displacements with tetrabutylammonium pyrophosphate (CH_3CN , 25°C , 2 h), ion exchange to the NH_4 salts, and chromatography on cellulose (yields 46–94%) [45]. The labeled FPPs were characterized by 500 MHz ^1H NMR and 162 MHz ^{31}P NMR spectra (D_2O , EDTA, ND_4OD). The ^{31}P NMR spectra displayed the typical pair of doublets for the diphosphate and the absence of appreciable amounts of inorganic pyrophosphate.

Incubation and product analysis

Incubations of the deuterium-labeled FPPs with recombinant TEAS, HPS, and CH_4 enzymes were conducted according to a literature procedure [19] with some modifications. Frozen solutions of recombinant proteins were stored at -78°C in a storage buffer of 50% glycerol, 25 mM Tris-HCl (pH 7.5), 2.5 mM MgCl_2 , 0.5 mM β -mercaptoethanol, 0.5 $\mu\text{g}/\text{mL}$ leupeptin, and 0.5 mM phenylmethylsulfonyl fluoride. The concentrations were generally 4–10 mg/mL. Stock solutions containing 200 mM Tris-HCl (pH 7.5), 40 mM MgCl_2 , and 14 μM labeled FPP were mixed in the ratio 1:1:0.66 (Tris- MgCl_2 /FPP) providing the final incubation buffers. Appropriate amounts of enzyme (0.13 mg) were added to 0.80 mL of the final incubation buffers in glass test-tubes with Teflon-lined caps. The solutions were incubated at 37°C for 15 min and cooled to 0°C . The sesquiterpene products were extracted with pentane (typically 2×0.3 – 0.75 mL) containing 0.018 mM α -cedrene as GC standard, a small amount (~ 10 – 15 μL) of heptane was added, and the combined extracts were concentrated under N_2 flow to ca. 20 μL in 1-mL, conical vials for GC and GC-MS analysis. Product yields determined by capillary GC varied considerably, between 2% (100 ng) and 30% (1.5 μg). EI GC-MS analyses for isotope content were conducted by fast scanning through m/z 190–210. In contrast, GC-MS analyses for olefin identification were performed with a full mass scan m/z 55–210.

Incubations of [$13,13\text{-}^2\text{H}_2$]FPP (1- d_2), and [$13,13,13\text{-}^2\text{H}_3$]FPP (1- d_3) with TEAS

Stock solutions of 200 mM Tris-HCl (pH 7.5), 40 mM MgCl_2 , and 14 μM labeled FPPs were prepared as described above [19]. Aliquots of the enzyme solutions (0.028 mL, 0.13 mg) were added to two identical solutions containing 0.17 mL of distilled H_2O and 0.80 mL of the final incubation buffers. The duplicate solutions were carefully inverted several times to ensure mixing, and were incubated at 37°C for 15 min. After cooling at 0°C for 5 min in an ice bath, 300 μL of pentane was added, and the mixtures were vortexed and centrifuged. GC analyses of the pentane layers using the response factor for the α -cedrene standard (0.0063 ng/area) determined the conversions to epiaristolochene to be 25% (1000 ng) and 4% (150 ng) for incubations with [$13,13\text{-}^2\text{H}_2$]FPP and [$13,13,13\text{-}^2\text{H}_3$]FPP, respectively. After separation of the pentane layers from the buffer solutions with glass pipettes, 10 μL of heptane was added, and the combined pentane/heptane layers were carefully concentrated with N_2 in 100- μL , cone-bottomed vials. Data from the isotope ratio GC-MS analyses are presented in Table 1.

Corrections for the contributions of incompletely labeled FPPs on the fragment mass intensities were nearly insignificant since the isotopic and geometric purities of all labeled farnesols and all labeled FPPs were high. An example correction for the amount of FPP- d_1 in FPP- d_2 follows. The 0.5% farnesol- d_1 detected by MS analysis in the farnesol- d_2 would increase the amount of monodeuterated olefin observed in the GC-MS analyses of the sesquiterpenes derived from incubations with the FPP- d_2 . The apparent amount of deuterium elimination needs to be corrected for this contribution. The measured intramolecular KIE of 4.3 (Table 1) reflects the relative rates of proton and deuterium elimination. The presence of two protons doubles the probability of their elimination with respect to deuterium. Thus of the 0.5% FPP- d_1 in FPP- d_2 , 0.45% is expected to be converted to the monodeuterio olefin [$4.3 + 4.3/(4.3 + 4.3 + 1) \times 0.5\%$], and this value was subtracted from the experimentally measured amount of dideuterio olefin in the calculation of the KIE. Similar calculations provided corrections amounting to 1–

2% changes on the KIEs shown in Tables 1 and 2. The deuterium content data in Tables 1–3 were derived directly from GC–MS analyses after correction for natural abundance carbon 13.

Incubations of large excesses (600×) of a 1:4.3 ($\pm 10\%$) mixture of unlabeled FPP and [12,12,12,13,13,13- $^2\text{H}_6$]-FPP (1- d_6) with TEAS and HPS were carried out to determine the intermolecular product KIEs (Table 1). The mixed FPP was prepared by combining portions of unlabeled and FPP- d_6 solutions. A sample of the mixture was analyzed by negative ion FAB MS (m/z 387(100), 381(23.6); 71.8% d_6 , 16.8% d_0) to determine the isotopic ratio of the unlabeled and labeled FPPs. The conversions of the mixed FPPs to olefinic product(s) and to farnesol were determined to be less than 1% by GC standardization with farnesol or α -cedrene. Thus, changes in the ratio of unlabeled FPP to FPP- d_6 in the unreacted diphosphate mixture were insignificant, and this assured that no depletion of unlabeled FPP occurred during the incubations.

Incubations in D_2O were performed by procedures similar to those described above for the small scale incubations in H_2O . (Table 2) Buffer solutions were prepared with D_2O except for the use of the acid (conc. HCl) used to adjust the pD, and the H_2O containing enzyme storage buffers. The pHs of the D_2O solutions were adjusted to 7.1 instead of 7.5 because of the 0.4 U difference between the pD and the measured pH for high percentage D_2O solutions [46]. The percentages of H_2O in the resulting D_2O buffers were determined by addition of anhydrous sodium acetate and integration of the ^1H NMR signals for H_2O and the acetate methyl group [46,47]. The isotopic content of the buffers prepared as described was 95–97% D_2O .

The location and stereochemical configuration of the deuterium incorporated into epiaristolochene were established by NMR analyses of the monodeuterio olefin produced by large scale TEAS incubations in D_2O . Incubations (74 \times 8 mL) containing 2.3 mg of TEAS, and extractions with 0.5 and 0.75 mL of a 0.018 mM cedrene solution in pentane, provided a total of 200 μg (GC) of epiaristolochene. The pentane extracts were filtered through a glass Pasteur pipette containing 1.0 g of silica gel. The fractions containing epiaristolochene as determined by TLC and GC analyses were combined and placed in a 5-mm NMR tube. Benzene- d_6 (0.75 mL) was added, the solution was carefully concentrated, and appropriate Wilmad Doty susceptibility plugs were inserted into the tube containing ca. 300 μL of benzene- d_6 . The percentage of D_2O in the incubation buffer was 96.3% by NMR standardization with anhydrous sodium acetate [47]. The isotopic content of the purified epiaristolochene was determined by GC–MS analysis to be 88.2% d_1 . The NMR assignments for epiaristolochene and the NMR analyses of epiaristolochene- d_1 isolated from the incubations in enriched D_2O are discussed in the following section.

Results

The results from GC–MS analyses of the sesquiterpene hydrocarbon products formed in the incubations of the various labeled forms of FPP with the recombinant TEAS, HPS, and chimeric CH_4 enzymes, and from incubations conducted in $\text{H}_2\text{O}+\text{D}_2\text{O}$ mixtures, are presented in Tables 1–3. The loss of a single deuterium ($\geq 99\%$) with FPP- d_3 establishes that the methyl-methylene eliminations leading to the germacrene A intermediate occur stereospecifically at the *cis*-terminal methyl group in all cases. The preferential transfers of hydrogen over deuterium from the *cis*- CHD_2 group of FPP- d_2 evident in the label content of products reveal substantial primary kinetic isotope effects ($k_{\text{H}}/k_{\text{D}} = 4.25\text{--}4.64$) in these methyl-methylene elimination reactions. In contrast TEAS and HPS showed at most small differences in the rates of cyclization of unlabeled substrate in a 1:4.3 mixture with FPP- d_6 bearing the heavier isotope in both terminal methyl groups. Nevertheless, the competitive intermolecular isotope effect of 1.33 determined for the reaction catalyzed by HPS is significantly greater than the estimated error range of ± 0.03 .

The enzyme-catalyzed conversions of FPP to sesquiterpene products in highly enriched D₂O (92–97%) were considerably lower than those in undeuterated medium according to GC analyses using α -cedrene as internal standard. Typical yields from incubations in D₂O were about 10%, compared to about 30% for incubations in H₂O. It is clear from the results listed in Table 2 that a considerable amount of deuterium is incorporated into epiaristolochene and premnaspirodiene (80–91% *d*₁) in the incubations in D₂O. The low level of isotope incorporation into epieremophilene (87 and 98% *d*₀) is attributed to the fact that deuterium addition to the 1,10 double bond of the germacrene A intermediate occurs on the same face as the proton (deuterium) elimination forming the 1,10 double bond in the product. The D1 β configuration of the deuterium incorporated in addition to germacrene A was established by NMR spectral analyses of the epiaristolochene-*d*₁ isolated from the large scale incubations in D₂O.

The ¹H NMR spectrum of a reference sample of epiaristolochene synthesized from capsidiol [9] in benzene-*d*₆ provided the greatest resolution for the proton resonances in the aliphatic region. The peaks for the 1 α and 1 β protons in the benzene-*d*₆ spectrum were identified by comparison of the coupling patterns and resonances of the same protons in CDCl₃ [9]. The signal at 2.24 ppm in deuterated benzene was assigned to H1 β (axial) because of the two large (13.5 Hz) coupling constants. The proton signal at 1.95 ppm had only one large (13.5 Hz) coupling constant and thus was expected to be H1 α (Eq. (1)).

The assignments for the two C1 protons, H1 β (2.24 ppm) and H1 α (1.95 ppm), were verified by homonuclear chemical shift correlation (COSY), heteronuclear multiple-quantum correlation (HMQC), and NOE spectra in benzene-*d*₆. NOE measurements (Fig. 1) with pulsing on the angular methyl (C15, 1.17 ppm) clearly demonstrated that the signal at 2.24 ppm was H1 β by the positive 2.1% enhancement. There also was a strong 7.7% enhancement at H1 α (1.97 ppm) from pulsing on H9 (5.55 ppm). Unambiguous assignments for the C1 protons are essential to elucidate the stereochemistry of the protonation and eliminations that occur in the cyclization of germacrene A to epiaristolochene.

The 115 MHz ²H NMR spectrum of epiaristolochene-*d*₁ accumulated from several large scale incubations of FPP with TEAS in 96% D₂O displays only one signal at 2.21 ppm that corresponds to deuterium located at H1 β (Fig. 2B). In the related 750 MHz ¹H NMR spectrum the peak for H1 β is missing, and the signal for H1 α is shifted upfield by 0.024 ppm and collapsed to a broad singlet (Fig. 2C). ¹H NMR spectra of unlabeled epiaristolochene and α -cedrene are shown in Figs. 2A and D for comparison. Also seen in the ¹H NMR spectrum (panel C) is a signal at 2.19 ppm from the added α -cedrene carrier. A 15% NOE enhancement was observed at 1.94 ppm upon irradiation at the C9 vinyl proton (5.53 ppm), verifying that the signal at 1.94 ppm is indeed from H1 α . Examination of the line shape near 1.94 ppm (H1 α) in the ²H NMR spectrum and measurement of the noise level showed that the facial selectivity of the deuterium incorporation was greater than 95:5 H1 β /H1 α .

The almost complete absence of deuterium label in epiaristolochene produced by incubations of (*S*)-[8-²H₁]FPP with TEAS and CH₄ establishes that the 1 β proton is eliminated in the formation of the endocyclic 9, 10 double bond of this sesquiterpene. (Table 3) This conclusion is reinforced by the complete retention of label in the epiaristolochene formed in incubations with the enantiomerically deuterated substrate. The retention of some deuterium label (5–8%) in the epiaristolochene obtained from (*S*)-[8-²H₁]FPP may be attributed to the presence of a small, unknown amount of (*R*)-[8-²H₁]FPP, together with the influence of a primary isotope effect that would enhance the proportion of epiaristolochene-*d*₁. The complete retention of deuterium in the epieremophilene and premnaspirodiene products are to be expected since both of the terminating eliminations occur at positions other than C-8 (FPP position). The decreased proportion of epiaristolochene and the increased proportion of epieremophilene observed with

substrate labeled in the pro-S position signify the occurrence of isotopically sensitive branching in the formation of these double bond isomers.

Discussion

The methyl-methylene eliminations that form the isopropenyl double bond of the enzyme-bound germacrene A intermediates take place at the *cis*-terminal methyl position with all three enzymes. The *cis*-selectivity of the elimination step leading to epiaristolochene had been deduced previously from the ^{13}C NMR spectrum and ^{13}C – ^{13}C couplings of labeled capsidiol obtained from incorporation of $[1,2-^{13}\text{C}_2]$ acetate into the phytoalexin in elicited pepper fruits [6]. It is clear that the transfers of protium or deuterium from the transient germacren-11-yl⁺ ion intermediate to the active site acceptors occur faster than rotation about the exocyclic C7–C11 sigma bond which would interchange the terminal methyl groups. Furthermore, the almost complete absence of any mono-deuterated products ($\leq 1\%$ d_1) indicates that the deuterium transfers are effectively irreversible. If exchange of the eliminated deuterium with the surrounding medium were fast, reprotonation would lead to incorporation of hydrogen and a decrease of the deuterium content. The absence of detectable amounts of trideuterated sesquiterpene products formed from FPP- d_3 is evidence against any re-incorporation of label in the further cyclization of germacrene A to the final bicyclic products. In contrast, efficient proton re-incorporations have been observed in the cyclizations catalyzed by pentalenene, abietadiene, and taxadiene synthases [48–51].

Similar *cis*-selectivity in methyl-methylene eliminations have been reported to occur in the cyclizations catalyzed by limonene synthases from *Citrus sinensis* and *Perilla frutescens* [52,53], and by aristolochene synthase from *A. terreus* [25]. Natural abundance ^2H NMR analysis of (+)-limonene from Florida navel oranges lead to the same conclusion [54]. Other examples of *cis*-selective eliminations have been observed in the biosynthesis of the sesquiterpene germacrene-2, 3-diol [55] and the triterpenes betulonic acid and lupeol [56,57]. In contrast the methyl-methylene eliminations that occur in the enantiospecific cyclizations of geranyl PP to limonene catalyzed by (+)- and (–)-pinene synthases from *Salvia officinales* take place almost randomly at both terminal methyl groups [52].

The sizeable intramolecular isotope effects observed for the methyl-methylene eliminations, $k_{\text{H}}/k_{\text{D}}$ 4.3–4.6, signify a substantial degree of C–H/C–D bond breaking in the transition states for proton/deuterium transfer. Rapid rotation of the CHD_2 group would allow equilibration of the transition states for proton and deuterium elimination and discrimination in favor of the lighter isotope. The magnitude of these intramolecular isotope effects are at the high end of the range of values reported in the literature for methyl-methylene eliminations in terpene synthase reactions, $k_{\text{H}}/k_{\text{D}} = 2.1$ – 5.9 . [52,54,58]. It is noteworthy that the values for the CH_4 chimeric enzyme are somewhat larger 4.4–4.6 than those determined for TEAS and HPS, 4.27 and 4.25.

The much smaller values of the intermolecular methylmethylene isotope effects, 1.03 ± 0.01 and 1.33 ± 0.03 , observed in the competitive cyclizations of unlabeled substrate and FPP- d_6 bearing deuterium in both terminal methyl groups (Table 1) provide evidence that the proton elimination steps have at most small effect on reaction rates. Nevertheless, the significant isotope depletion observed in premnaspirodiene with HPS is probably associated with a β -deuterium isotope effect on the formation of the germacradien-11-yl⁺ ion in the macrocyclization step. It is well established that substitutions by deuterium in methyl groups adjacent to the carbocation site have substantial rate-retarding effects (ca. 10% per deuterium atom) on $\text{S}_{\text{N}}1$ solvolysis reactions [59,60]. The decreased stability of the carbocation intermediates is attributed to the reduced capacity of the C–D bonds to stabilize the positive

charge by hyperconjugation. Similar secondary isotope effects are associated with the rates of enzyme-catalyzed cyclizations of geranyl PP to cyclic monoterpenes [52,58].

Kinetic experiments with TEAS and HPS, as well as those with the chimeric enzymes CH₃ and CH₄, lead to the minimal mechanism shown in Eq. (1) below [22,24]. The rate constants k_2 and k_3 represent the rates at which products are formed and released to complete the catalytic cycle. It was concluded that the final step represented by k_3 is overall rate-limiting, and that this step may reflect either the rate of release of the hydrocarbon product(s) alone, or a composite of rates including a partially limiting chemical step (or steps) and product release. Rapid quench experiments indicated that $k_{-1} \gg k_2$, i.e. binding of FPP into the E·S complex is rapid and reversible under the conditions used, and further that $k_{\text{cat}}/K_M = k_1k_2/(k_1 + k_2) \cong k_2/K_D$ and $k_{\text{cat}} \cong k_3$ as shown in Eq. (2).



$$\frac{k_{\text{cat}}}{K_M} = \frac{k_1k_2}{(k_{-1} + k_2)} \approx \frac{k_2}{K_D} \text{ and } k_{\text{cat}} \approx k_3 \quad (2)$$

Some brief speculations follow about plausible molecular mechanisms and the location of the isotopically sensitive event in the multi-step processes. The discrimination in the competition between deuterated and non-deuterated FPP is a consequence of the isotope effect on k_{cat}/K_M [61]. Since the k_2 step in the minimal mechanism is irreversible, the KIE observed with FPP-*d*₆ and HPS in the competition experiments must be expressed at this stage. It seems reasonable to assume on the basis of average bond energies that the initial farnesyl → germacradienyl cyclization is irreversible ($\Delta H_{\text{BE}} \cong -20$ kcal/mol). One possibility is that heterolysis of the C–O bond of HPS-bound FPP occurs simultaneously with participation of the C10–C11 double bond, and consequently with some development of positive charge at C11 in the transition state represented by k_2 . Alternatively this step might involve relatively rapid and reversible dissociation of FPP to an enzyme-bound farnesyl⁺/OPP[−] ion pair that cyclizes relatively slowly to the germacradienyl⁺ intermediate. In either case, k_2 in Eq. (1) measures the rate of HPS-catalyzed cyclization of FPP to the germacrene A intermediate.

The absence of a significant discrimination against FPP-*d*₆ in the same competition experiments with TEAS reveals substantially altered kinetics that result in masking of the remote KIE. One explanation is that ionization of FPP to a similar TEAS-bound farnesyl⁺/OPP[−] ion pair is now relatively slow and irreversible, and is followed by a more rapid macrocyclization event. In this case, C–C bond formation and the attendant remote KIE would occur after substrate is irreversibly committed to germacrene A. Alternatively it seems conceivable that the k_2 step might reflect a relatively slow, irreversible conformational change of the initial TEAS·FPP complex. For example, if FPP were initially bound in an extended, unproductive conformation in E·S, a re-orientation would be necessary to bring the polyene chain into position for cyclization to take place. Thus, the possibility of a second E·S complex on the path to E·P in Eq. (1) would be implicated. It should be noted that these competition experiments were conducted at very high FPP concentrations (ca. 2 M) to ensure low conversions. Under these conditions it seems possible that the minimal mechanism and kinetic constants in Eqs. (1) and (2) [22,24] could be altered in the competitive incubations of FPP-*d*₀ and FPP-*d*₆ with TEAS.

The 1β stereochemistry of the deuterium incorporated into epiaristolochene-*d*₁ was proven by NMR analysis of the product formed when the incubation of FPP with TEAS was conducted

in highly enriched D₂O. Thus, the C–D bond is formed on the re face of C-1 of the 1,10 double bond of the germacrene A intermediate. Protonation or deuteration of an isolated C=C double at neutral pH must have a relatively high activation energy. Thus it seems likely that the deuteron transfer onto germacrene A occurs simultaneous with transannular cyclization onto the opposing 4,5 double bond to form directly the eudesmyl ion intermediate **10A**. The enhanced reactivity of germacrene A, and the ease with which it undergoes proton-induced cyclization, are evident in the silica gel-induced cyclization of the triene to (–)-selin-11-en-4-ol at room temperature, albeit from the more stable chair–chair conformation that results in the formation of a *trans*-fused eudesmane structure [62]. The boat-chair conformation of the enzyme-bound germacrene A would have the two ring double bonds aligned in close proximity to allow a concerted deuteration-cyclization process, and the observed 1β stereochemistry is appropriate for a coupled antiperiplanar addition-cyclization mechanism. The partial acquisition of four strong sigma C–C bonds from the two C=C double bonds would clearly provide added driving force for this critical step in the multi-step mechanism. In the absence of any direct evidence, we suppose that germacrene A is an intermediate in the reactions catalyzed by HPS and CH₄ cyclases, and furthermore it seems reasonable to assume that the proton transfer steps initiating the conversions to the bicyclic products occur with the same 1β stereochemistry established for TEAS.

The incubation solutions used for the deuterium incorporation experiments discussed above also contained a small, precisely determined amount of H₂O, i.e., 3–8%. The accurately known H₂O–D₂O solvent composition, together with the deuterium content of the products measured by GC–MS, provided the data needed to calculate the product isotope effects shown in Table 2. The magnitudes of the solvent isotope effects, 1.7–2.9, are similar to those determined for *Abies grandis* abietadiene synthase (1.9) [47], *E. coli* tryptophan-indole lyase (1.8) [63], and *Streptomyces* R61-DD peptidase (2.2–2.7) [64]. Although, many factors affect product isotope effects [46], it seems likely that the H/D discrimination occurs in the protonation-cyclization of germacrene A. If we assume that H/D exchange of the medium with the proximal proton donor is fast, the immediate deuterium transfer to germacrene A appears to be substantially slower than the competing proton transfer.

All of the reactions catalyzed by the three enzymes are terminated by methylene-methine eliminations that form the endocyclic double bonds of the bicyclic products. The stereochemistry of the proton transfer from C-9 of the eremophilanyl ion intermediate **11** that leads to epiaristolochene was determined directly from the deuterium content of the product formed in incubations of the stereospecifically labeled substrates (*S*)- and (*R*)-[8-²H₁]FPP with TEAS and CH₄. The data in Table 3 show clearly that deuterium is lost from substrate bearing label in the pro-*S* position, and the isotope is retained when the label resides in the pro-*R* position. It follows that the 9β proton *cis* to the angular methyl group is eliminated to the extent of 92–95% in forming the 9,10 double bond of epiaristolochene. The relatively small amounts (5–8%) of epiaristolochene-*d*₁ also detected in the GC–MS analyses probably arise from low levels of contamination by the enantiomeric FPP-*d*₁ since its proportion with respect to epieremophilene-*d*₀ would be magnified by the more favorable elimination of hydrogen. The exact enantiomeric purities of the labeled intermediates **24-d**₁ and **18-d**₁ after the Biellmann coupling were not determined, and contamination by 2–3% of the enantiomers would be sufficient to account for the results when the magnifying influence of a primary isotope effect is considered.

The 2.4-fold increase in the proportion of epieremophilene in the products formed from (*S*)-[8-²H₁]FPP by TEAS compared to that obtained with unlabeled substrate (6.7% vs. 15.8%), and the very similar decrease in the proportion of epiaristolochene formed from the CH₄ enzyme with the same labeled substrate (18.5 vs. 7.9%), indicate the influence of a primary isotope effect on the product composition. (Table 3) Complementary changes are also apparent

in the relative amounts of the major products from (*S*)-[8-²H₁]FPP with the two enzymes, i.e., epiaristolochene from TEAS and epieremophilene from CH₄. It is evident that the isomeric products arise by competitive proton eliminations from the common eudesmyl carbocation intermediate **11**. The presence of deuterium in the 9β position slows down the rate of the elimination producing epiaristolochene and the proportion of epieremophilene increases.

In contrast to the high deuterium content of epiaristolochene produced in the incubations conducted in highly enriched D₂O, the epieremophilene also formed in the reactions catalyzed by TEAS and CH₄ was mostly undeuterated (87 and 98% *d*₀, Table 2). Since the deuterium transfer would have occurred on the re (β) face of the 1,10 double bond of germacrene A, it is clear that the 1β proton *cis* to the angular methyl group must be the one eliminated in the formation of endocyclic double bond of epieremophilene, i.e., the same face as the elimination producing epiaristolochene. On the other hand, the premnaspirodiene obtained in the incubations with HPS and CH₄ in D₂O was largely monodeuterated (91 and 80%), despite the fact that the elimination must have occurred at the site bearing deuterium. If we assume that the protonation of germacrene A catalyzed by HPS and CH₄ takes place with the same 1β stereochemistry established for TEAS catalysis, then the 1α proton, *cis* to the opposing methyl substituent on the six-membered ring, is eliminated in the formation of premnaspirodiene.

The stereochemical conclusions drawn from the labeling experiments, together with analogies to other terpene synthase mechanisms, provide the basis for the conformational depictions of the intermediates and stereochemical course of the individual reactions catalyzed by the three cyclases presented in Scheme 5. Folding of the acyclic polyene chain of the FPP substrate into boat-chair-like conformation (**1**) sets the stage for the macrocyclization initiated by heterolysis of the C–O bond of the allylic diphosphate. The resulting germacren-11-yl carbocation (not shown) undergoes rapid CH₃ → CH₂ elimination by proton transfer from the *cis*-terminal methyl group to an active site base to form the isopropenyl group. The two internal double bonds of the neutral germacrene A intermediate in a boat-chair conformation **9** are aligned for protonation on the exterior (re) face of the 1,10 double bond and for concerted cyclization to generate the *cis*-eudesm-4-yl ion **10A**, probably initially in a boat-chair conformation resembling that of its cyclodecadiene precursor. Hydride shift from C-5 to C-4 generates the eudesm-5-yl branch point intermediate **10B** in the consolidated scheme.

The chair–chair conformation of ion **10B** predisposes the angular methyl group for a stereoelectronically favorable rearrangement from C-10 to C-5 to form eremophilene-10-yl ion **11**. Competitive eliminations of the axial 1β and 9β hydrogens then give rise to epieremophilene and epiaristolochene. Formation of the spiro[4.5]decane nucleus of premnaspirodiene by a stereoelectronically favorable Wagner–Meerwein rearrangement must be preceded by conformational inversion of the isopropenyl-bearing ring, i.e., **10B** → **10C**. With the C-9 methylene group in an axial position in conformer **10C**, the fused-spiro rearrangement can take place to generate vetispirenyl ion **12**. Transfer of the axial 1α proton to an active site acceptor completes the path to premnaspirodiene (**5**).

The consistent stereochemistry and isotope effects associated with the proton eliminations that occur in the active sites of TEAS, HPS, and CH₄ in the formation of all three sesquiterpene products indicate very similar mechanisms, and probably participation by the same active acids and bases in each case. The CH₃ → CH₂ eliminations in the initial cyclizations generating germacrene A all occur at the *cis*-terminal methyl groups, a stereo bias in common with many other monoterpene and sesquiterpene cyclization reactions. The relatively large primary KIEs signify similar, product-like transition states for these proton transfers steps. The opposite stereochemistry of the final CH₂ → CH eliminations forming the endocyclic double bonds of epiaristolochene and epieremophilene compared to that of premnaspirodiene reflects quite different orientations of the eremophilenyl and vetispirenyl carbocations **11** and **12** in the

catalytic sites with respect to the active site bases of TEAS and HPS that serve as proton acceptors. None-the-less the same facial biases are seen in the three competing reactions catalyzed by the chimeric CH₄ enzyme.

Further research is needed to identify the enzyme bases that participate in the proton elimination steps, to establish the precise orientations of the short-lived intermediates in the active sites, and to characterize the enzyme-intermediate contacts and dynamics responsible for channeling the carbocations to the eremophilane and vetispirane products by these similar sesquiterpene synthases.

Acknowledgments

The authors thank R. Milberg, S. Mullen, and F. Sun for assistance with GC–MS analyses; V. Mainz, F. Lin, and P. Molitor for assistance with NMR spectroscopy; D.E. Cane and P.O' Maille for helpful comments on the ms.; and the National Institutes of Health (UIUC, GM 13956) for financial support. J.P. Noel is an investigator of the Howard Hughes Medical Institute.

This article is dedicated to Professor Rodney Croteau on the occasion of his 60th birthday.

References

1. Cane, DE. Comprehensive Natural Products Chemistry. Barton, D.; Nakanishi, K.; Meth-Cohn, O.; Cane, DE., editors. Vol. 2. Elsevier; Amsterdam: 1999. Chap. 6
2. Cane DE. Chem Rev 1990;90:1089–1103.
3. Brooks CJW, Watson DG. Nat Prod Rep 1985;2:427–460.
4. Brooks CJW, Watson DG. Nat Prod Rep 1991;8:367–390. [PubMed: 1787921]
5. Sharma, RP.; Salunkhe, DK. Mycotoxins and Phytoalexins. CRC Press; Boca Raton: 1991.
6. Baker FC, Brooks CJW. Phytochemistry 1976;15:689–694.
7. Hoyano Y, Stoessel A, Stothers JB. Can J Chem 1980;58:1894–1896.
8. Whitehead IM, Threlfall DR, Ewing DF. Phytochemistry 1989;28:775–779.
9. Whitehead IM, Ewing DF, Threlfall DR, Cane DE, Prabhakaran PC. Phytochemistry 1990;29:479–482.
10. Birnbaum GI, Stoessel A, Grover SH, Stothers JB. Can J Chem 1974;52:993–1005.
11. Zhao Y, Schenk DJ, Takahashi S, Chappell J, Coates RM. J Org Chem 2004;69:7428–7435. [PubMed: 15497966]
12. Takahashi S, Zhao Y, O'Maille PE, Greenhagen BT, Noel JP, Coates RM, Chappell J. J Biol Chem 2005;280:3686–3696. [PubMed: 15522862]
13. Murai A, Yoshizawa Y, Katsui N, Sato S, Masamune T. Chem Lett 1986:771–772.
14. Murai A, Sato S, Osada A, Katsui N, Masamune T. J Chem Soc Chem Commun 1982:32–33.
15. Whitehead IM, Atkinson AL, Threlfall DR. Planta 1990;182:81–88.
16. Rao CB, Raju GVS, Krishna PG. Ind J Chem Sect B 1982;21B:267–268.
17. Hwu JR, Wetzel JM. J Org Chem 1992;57:922–928.
18. Zee SH, Chou SY, Chinese J. Chem Soc (Taipei, Taiwan) 1990;37:191–195.
19. Back K, Chappell J. J Biol Chem 1995;270:7375–7381. [PubMed: 7706281]
20. Back K, Yin S, Chappell J. Arch Biochem Biophys 1994;315:527–532. [PubMed: 7986100]
21. Back K, Chappell J. Proc Natl Acad Sci USA 1996;93:6841–6845. [PubMed: 8692906]
22. Mathis JR, Back K, Starks C, Noel J, Poulter CD, Chappell J. Biochemistry 1997;36:8340–8348. [PubMed: 9204881]
23. Starks CM, Back K, Chappell J, Noel JP. Science 1997;277:1815–1820. [PubMed: 9295271]
24. Rising KA, Starks CM, Noel JP, Chappell J. J Am Chem Soc 2000;122:1861–1866.
25. Cane DE, Prabhakaran PC, Oliver JS, McIlwaine DB. J Am Chem Soc 1990;112:3209–3210.
26. Cane DE, Prabhakaran PC, Salaski EJ, Harrison PHM, Noguchi H, Rawlings BJ. J Am Chem Soc 1989;111:8914–8916.

27. Cane DE, Tsantrizos YS. *J Am Chem Soc* 1996;118:10037–10040.
28. Still CW, Kahn M, Mitra A. *J Org Chem* 1978;43:2923–2925.
29. Morimoto Y, Matsuda F, Shirahama H. *Tetrahedron* 1996;52:10609–10630.
30. Yee NKN, Coates RM. *J Org Chem* 1992;57:4598–4608.
31. Ravn MM, Jin AQ, Coates RM. *Eur J Org Chem* 2000:1401–1410.
32. Jin Q, Williams DC, Hezari M, Croteau R, Coates RM. *J Org Chem* 2005;70 ASAP.
33. Clarke HT, Hartman WW. *Org Synth Coll* 1993;1:233–234.
34. Still WC, Gennari C. *Tetrahedron Lett* 1983;24:4405–4408.
35. Coates RM, Ley DA, Cavender PL. *J Org Chem* 1978;43:4915–4922.
36. Welch SC, Walters MEJ. *J Org Chem* 1978;43:4797–4799.
37. Schenk, DJ. PhD Dissertation. University of Illinois; Urbana, IL: 2000. Diss. Abstr. B; Order No. DA 9990130, 61(2000) 5334.
38. Corey EJ, Cane DE, Libit LJ. *J Am Chem Soc* 1971;93:7016–7021.
39. Corey EJ, Achiwa KJ. *Org Chem* 1969;34:3667–3668.
40. Davisson VJ, Woodside AB, Neal TR, Stremmer KE, Muehlbacker M, Poulter CD. *J Org Chem* 1986;51:4768–4779.
41. Gerlach H, Zagalak BJ. *J Chem Soc Chem Commun* 1973:274–275.
42. Gerlach H, Kappes D, Boeckman RK Jr, Maw GN. *Org Synth Coll* 1998;9:151–154.
43. Crandall JK, Pradat C. *J Org Chem* 1985;50:1327–1329.
44. Collington EW, Meyers AI. *J Org Chem* 1971;36:3044–3045.
45. Woodside AB, Huang Z, Poulter CD. *Org Synth Coll* 1993;8:616–620.
46. Schowen KB, Schowen RL. *Methods Enzymol* 1982;87:551–606. [PubMed: 6294457]
47. Ravn, MM. PhD Thesis. University of Illinois; Urbana, IL: 2000.
48. Cane DE, Oliver JS, Harrison PHM, Abell C, Hubbard BR, Kane CT, Lattman R. *J Am Chem Soc* 1990;112:4513–4524.
49. Ravn MM, Coates RM, Jetter R, Croteau RB. *J Chem Soc Chem Commun* 1998:21–22.
50. Lin X, Hezari M, Koeppe AE, Floss HG, Croteau R. *Biochemistry* 1996;35:2968–2977. [PubMed: 8608134]
51. Williams DC, Carroll B, Jin Q, Rithner C, Lenger SR, Floss HG, Coates RM, Williams RM, Croteau R. *Chem Biol* 2000;7:969–977. [PubMed: 11137819]
52. Pyun HJ, Coates RM, Wagschal KC, McGeady P, Croteau RB. *J Org Chem* 1993;58:3998–4009.
53. Suga T, Hiraga Y, Mie A, Izumi S. *J Chem Soc Chem Commun* 1992:1556–1558.
54. Leopold MF, Epstein WW, Grant DM. *J Am Chem Soc* 1988;110:616–617.
55. Birnbaum GI, Huber CP, Post ML, Stothers JB, Robinson JR, Stoessel A, Ward EWB. *J Chem Soc Chem Commun* 1976:330–331.
56. Botta, L. PhD Thesis. ETH; Zurich, Switzerland: 1968.
57. Guglielmietta, L. PhD Thesis. ETH; Zurich, Switzerland: 1962.
58. Wagschal KC, Pyun HJ, Coates RM, Croteau R. *Arch Biochem Biophys* 1994;308:477–487. [PubMed: 8109978]
59. Streitwieser, A, Jr. *Solvolytic Displacement Reactions*. McGraw-Hill; New York: 1962. p. 98-102.
60. Shiner VJ Jr. *J Am Chem Soc* 1953;75:2925–2929.
61. Walsh, C. *Enzymatic Reaction Mechanisms*. Freeman; San Francisco: 1979. p. 118-123.
62. Adio AM, Paul C, Tesso H, Kloth P, König WA. *Tetrahedron Asymmetr* 2004;15:1631–1635.
63. Rickert KW, Klinman JP. *Biochemistry* 1999;38:12218–12228. [PubMed: 10493789]
64. Adediran SA, Pratt RF. *Biochemistry* 1999;38:1469–1477. [PubMed: 9931012]

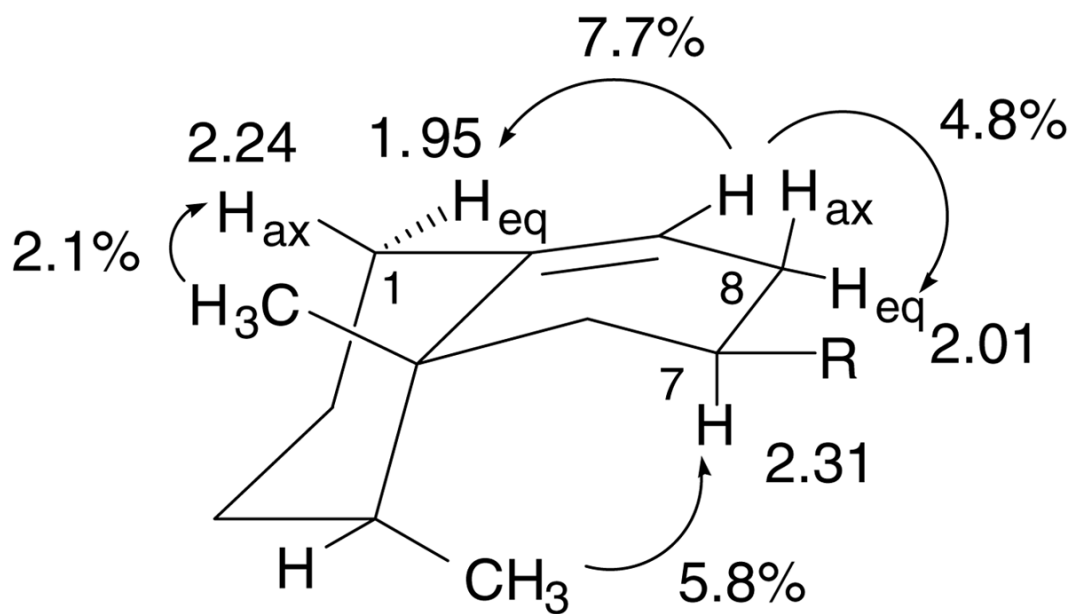


Fig. 1. NOEs determined for epiaristolochene in benzene-*d*₆ following irradiations at the vicinal methyl groups (δ 0.98, 1.17) and the C-9 vinyl proton (δ 5.55), and the resulting chemical shift assignments for H1 β (H_{ax}), H1 α (H_{eq}), and H8 α (H_{eq}) (δ 2.24, 1.95, and 2.31).

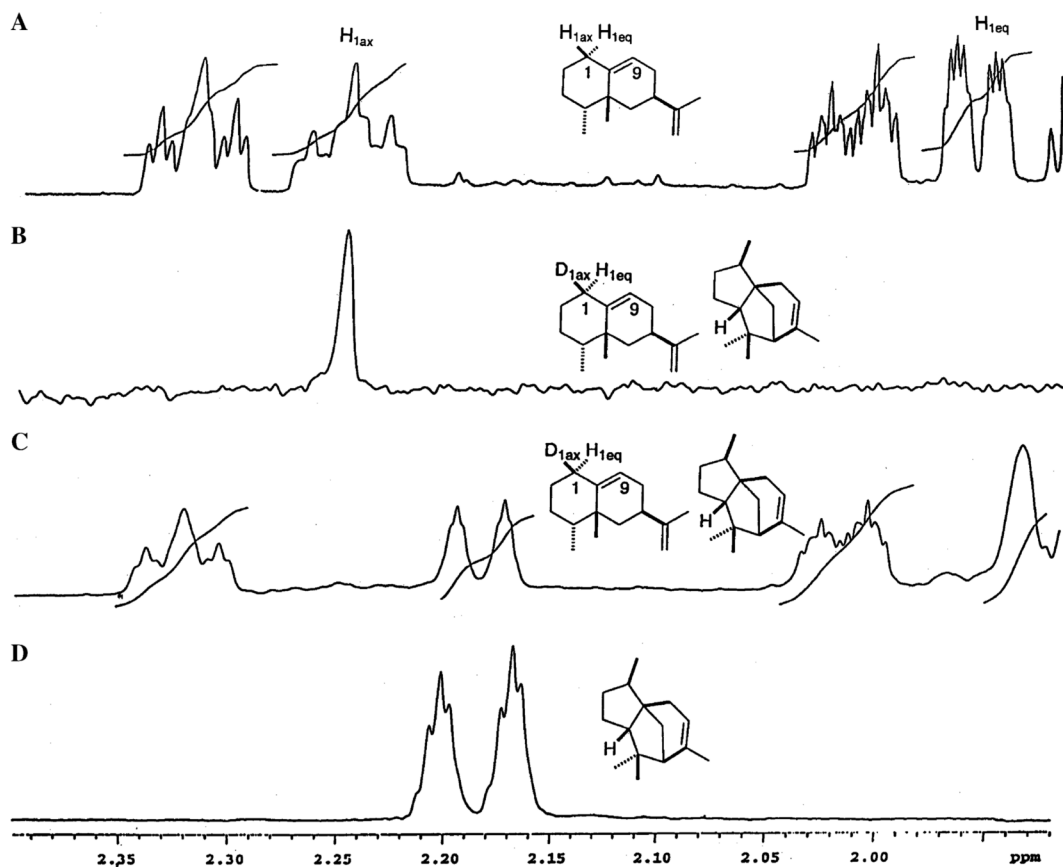
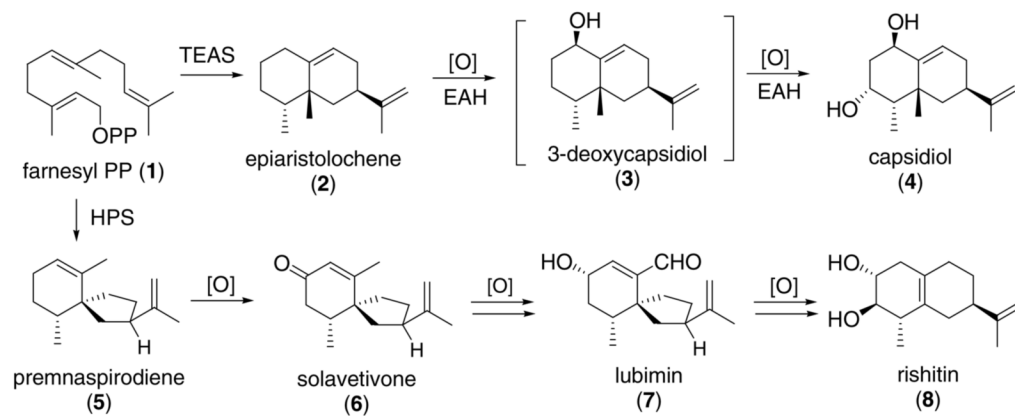
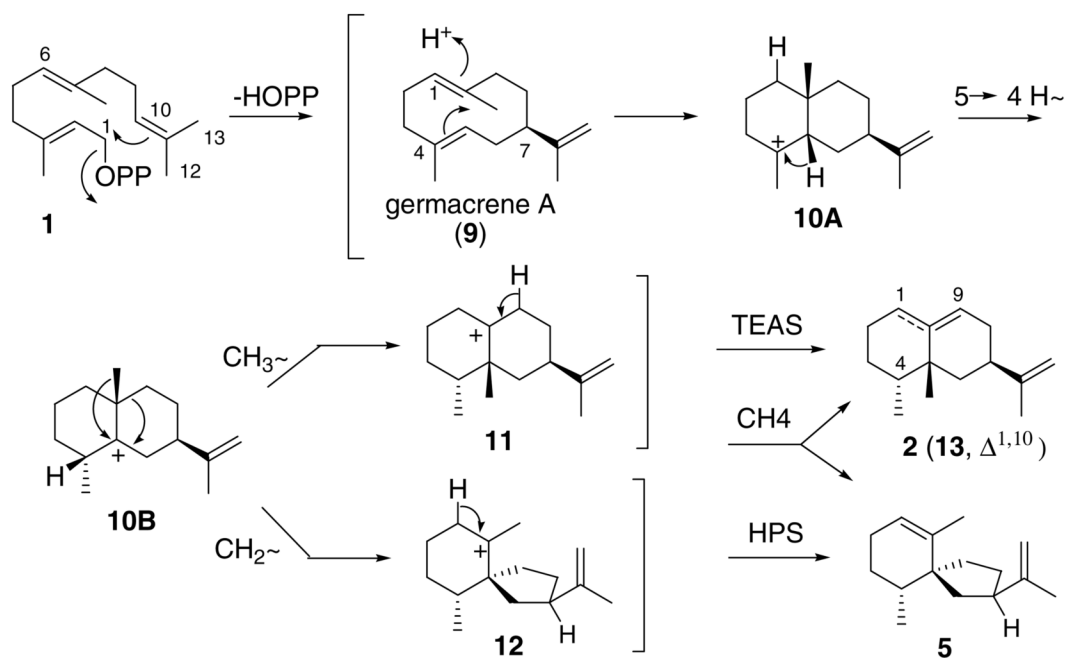


Fig. 2. The δ 1.92–2.40 regions of the 750 MHz ^1H and 115 MHz ^2H NMR spectra of epiaristolochene, an epiaristolochene- d_1 + α -cedrene mixture, and α -cedrene in benzene- d_6 : (A) ^1H NMR spectrum of unlabeled epiaristolochene, (B) ^2H NMR spectrum of epiaristolochene- d_1 isolated from the incubation of FPP with TEAS in D_2O in the presence of added α -cedrene carrier; (C) ^1H NMR spectrum of the same epiaristolochene- d_1 + α -cedrene mixture; (D) ^1H NMR spectrum of α -cedrene alone. The appearance of the signal at δ 2.19 in the ^2H NMR spectrum (B), and the absence of the corresponding peak in the ^1H NMR spectrum (C), prove that the deuterium in epiaristolochene- d_1 resides in the $\text{H}1\beta$ position.

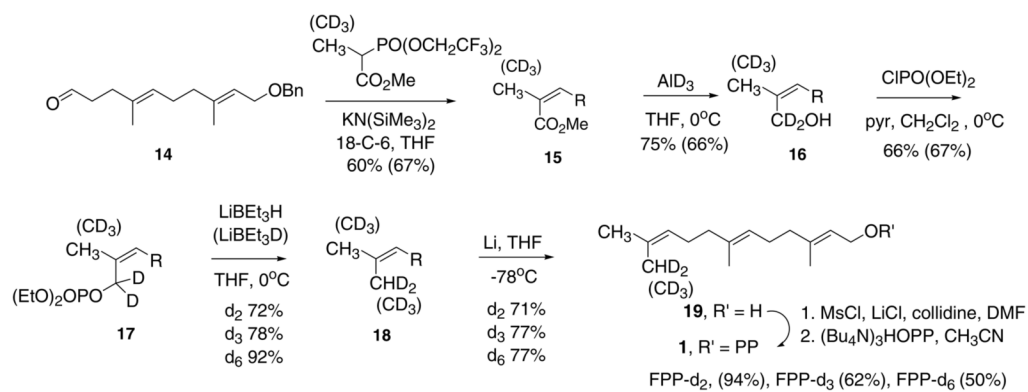
**Scheme 1.**

Biosynthesis of the sesquiterpene phytoalexins capsidiol (4), solavetivone (6), lubimin (7), and rishitin (8) from (*E,E*)-farnesyl diphosphate (1) by way of epiaristolochene (2) and premnaspirodiene (5).

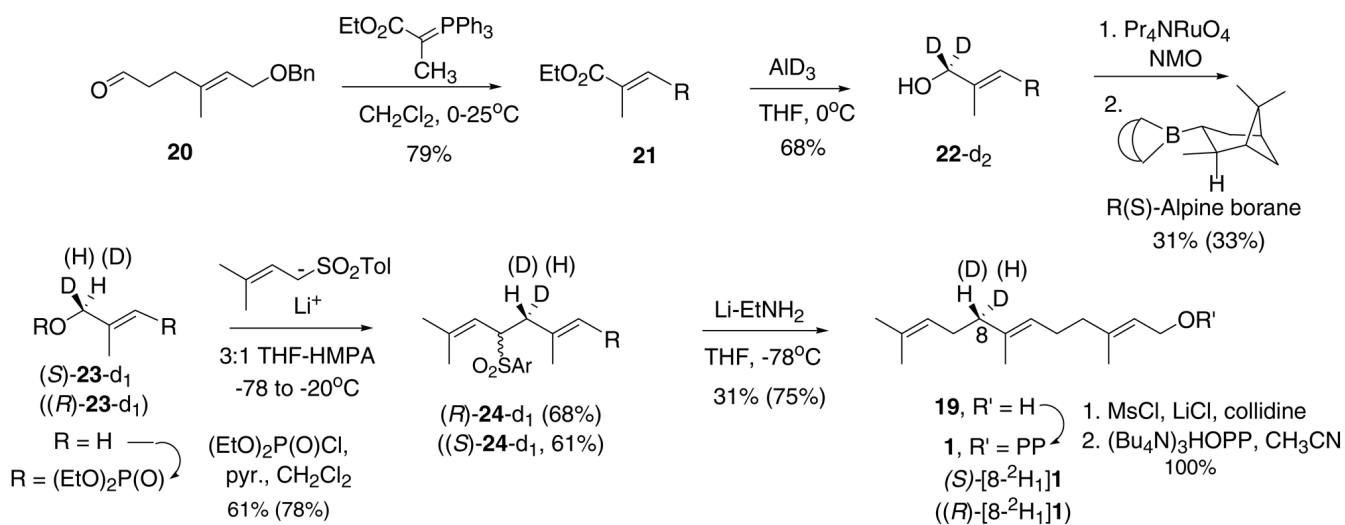


Scheme 2.

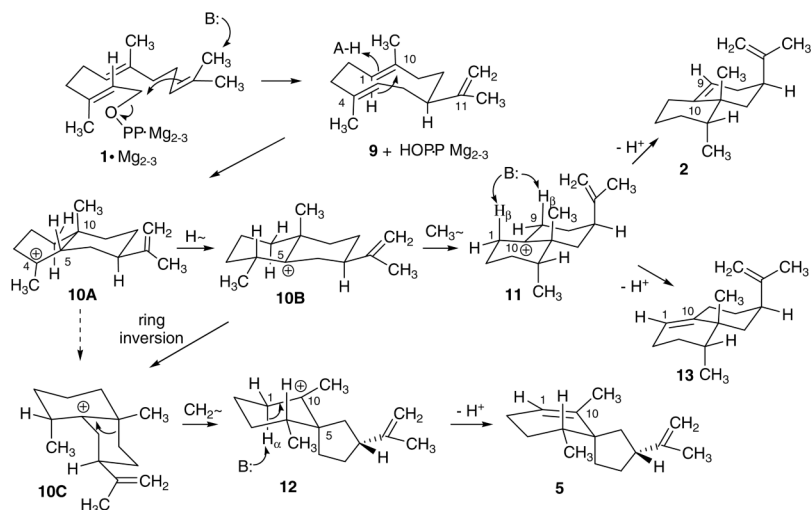
Proposed mechanisms for the cyclizations of (*E,E*)-farnesyl diphosphate (**1**) to epiaristolochene (**2**), epi-eremophilene (**13**), and premnaspirodienone (**5**) catalyzed by the respective synthases TEAS, HPS, and the CH₄ hybrid. The reactions proceed through germacrene A (**9**), and isomeric eudesmyl (**10A** and **10B**), epi-eremophilenyli (**11**), and vetispiirenyli (**12**) carbocation intermediates. In the case of TEAS, angular methyl migration is favored along the upper branch to the fused ring product whereas in the case of HPS ring methylene rearrangement on the opposite face and proton elimination at C1 lead to the spiro[5.4]decane product. The CH₄ mutant form affords a mixture of both products, together with the double bond isomer epi-eremophilene (**13**).

**Scheme 3.**

Synthesis of farnesyl diphosphates labeled with deuterium in the terminal methyl groups: [13,13-²H₂]**1**, [13,13,13-²H₃]**1**, and [12,12,12,13,13,13-²H₆]**1**. R=CH₂CH₂C(CH₃)=CHC(CH₃)=CHCH₂OBn.

**Scheme 4.**

Synthesis of farnesyl diphosphates labeled with deuterium in the pro-S and pro-R at C-8: (S)-[8-²H₁]**1** and (R)-[8-²H₁]**1**. R = (E,E)-CH₂CH₂C(CH₃)=CHCH₂OBn.

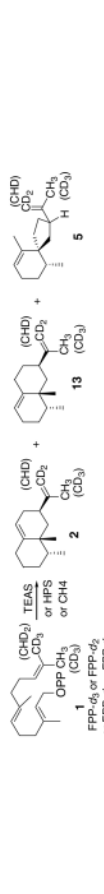


Scheme 5.

Conformational representations of FPP substrate, germacrene A intermediate, carbocation intermediates, and sesquiterpene products in the multi-step mechanism proposed for the overall reactions catalyzed by the TEAS, HPS, and CH₄ enzymes.

The deuterium content of the sesquiterpene products obtained from incubations of [$13,13,13\text{-}^2\text{H}_3$]FPP (**1-d₃**), [$13,13\text{-}^2\text{H}_2$]FPP (**1-d₂**), and a 1:4:3 mixture of unlabeled FPP and [$12,12,12,13,13\text{-}^2\text{H}_6$]FPP (**1-d₀ + 1-d₆**) with TEAS, HPS, and CH_4 recombinant enzymes is presented

Table 1



Enzyme	Product	Substrates, product deuterium contents(%), and isotope effects								
		FPP-d ₃		FPP-d ₂		FPP-d ₀ + FPP-d ₆		d ₀	d ₅	k _H /k _D
		d ₂	d ₃	d ₁	d ₂	k _H /k _D	d ₀			
TEAS	Epiaristolochene (2)	99.5	0.5	32.0	67.2	4.27 ± 0.04	18.7	79.6	1.03 ± 0.01	
HPS	Prennaspiprodien (5)	99.6	0.4	32.2	67.3	4.25 ± 0.08	23.0	75.3	1.33 ± 0.03	
CH_4	Epiaristolochene	99.0	1.0	30.2	68.8	4.64 ± 0.07				
	Epiemophilene (13)	99.7	0.3	31.2	67.9	4.43 ± 0.02				
	Prennaspiprodien	99.6	0.4	30.8	68.6	4.53 ± 0.01				

The near quantitative formation of deuterated products from FPP-d₃ reveals that the $\text{CH}_3 \rightarrow \text{CH}_2$ elimination occurs essentially exclusively at the *cis*-terminal methyl group. The intramolecular kinetic isotope effects (k_H/k_D) associated with the $\text{CH}_3 \rightarrow \text{CH}_2$ elimination were calculated from the deuterium content data of products from FPP-d₂. The corresponding intermolecular kinetic isotope effects (k_H/k_D) were deduced from the ratios of undeuterated and pentadeuterio products obtained from the FPP-d₀ + FPP-d₆ mixture.

Table 2

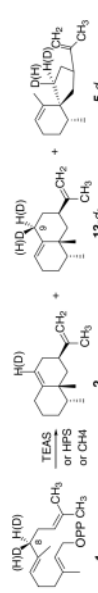
The deuterium content of sesquiterpene products isolated from incubations of recombinant TEAS, HPS, and CH₄ enzymes in a highly enriched D₂O medium is presented

Enzyme	D ₂ O (%)	Product	d ₀ (%)	d ₁ (%)	k _H /k _D
TEAS	95	Epiaristolochene (2)	9	91	2.7
		Epiremophilene (13)	87	12	
HPS	97	Premnaspirodienene (5)	9	91	2.7
CH ₄	92	Epiaristolochene	13	87	1.7
		Epiremophilene	98	2	
		Premnaspirodienene	20	80	2.9

The solvent isotope effects shown were calculated from the H₂O/D₂O ratios in the incubation medium and the deuterium incorporation into the products. The low level of deuterium incorporation into epiremophilene (13, Δ¹(10) isomer of 2) is a consequence of the deuterium addition and elimination occurring on the same β face of position 1.

The relative proportions of sesquiterpene products obtained from incubations of unlabeled substrate and substrate bearing isotope label in the pro-S and pro-R position, (S)- and (R)-[8-²H₁]FPP, with TEAS and CH₄ enzymes, and the deuterium content of the products from the labeled substrates, are presented

Table 3



Enzyme	Product	FPP-d ₀			(S)-[8- ² H ₁]FPP			(R)-[8- ² H ₁]FPP		
		%	d ₀	d ₁	%	d ₀	d ₁	%	d ₀	d ₁
TEAS	Epiaristolochene (2)	93.3 ± 0.4	84.2 ± 0.4	95.3	4.7	90.3 ± 0.3	0	100.0		
	Epierepholite (13)	6.7 ± 0.3	15.8 ± 0.2	0	100.0	9.7 ± 0.3	0	100.0		
CH ₄	Epiaristolochene	18.5 ± 0.2	7.9 ± 0.1	91.6	8.4	17.1 ± 0.1	0	100.0		
	Epierepholite	45.1 ± 0.2	52.1 ± 0.1	0	100.0	46.1 ± 0.6	0	100.0		
	Premnaspirodien (5)	29.7 ± 0.3	31.9 ± 0.1	0	100.0	30.0 ± 0.5	0	100.0		

A small peak for an unknown sesquiterpene (7%) was present in the GCs of the CH₄ products. The results show predominant elimination of the H_S deuterium or hydrogen in forming the 9,10 double bond of epiaristolochene with both enzymes. Complete retention of deuterium is observed in the other products because the final proton eliminations occur at other positions. The proportion of epiaristolochene-d₀ is decreased and that of epierepholite-d₁ is increased substantially with (S)-[8-²H₁]FPP as substrate.